Imaging of sand-pile interface submitted to a high number of loading cycles

J. Doreau-Malioche, G. Combe, J.B. Toni & G. Viggiani
Univ. Grenoble Alpes, CNRS, Grenoble INP (Institute of Engineering Univ. Grenoble Alpes), 3SR, Grenoble, France

M. Silva
Departamento de Obras Civiles
Universidad Técnica Federico Santa María, Valparaíso, Chile

ABSTRACT: The mechanisms occurring on a micro-scale at sand-pile interface during axial displacement-controlled cyclic loading were analysed quantitatively using x-ray tomography and a grain-based approach of three dimensional digital image correlation. The tests were performed in a mini-calibration chamber using a range of values of cyclic amplitudes and number of cycles. The results were found to be consistent with those obtained in a previous study carried out in a large calibration chamber, at Laboratoire 3SR, in France. The macroscopic response of sand-pile interface showed a two-regime evolution during cycles, with a non-negligible increase of shaft resistance in the latter regime. The test conditions are not representative of real engineering applications, where piles supporting bridges, tidal or wind turbines have to safely sustain severe load-controlled cycles. However, advanced image analysis sheds light on the mechanisms controlling the macroscopic behaviour of the sand-pile interface in each regime.

1 INTRODUCTION

The mechanisms controlling the macroscopic behaviour of sand-pile interface during pile installation and cyclic loading are complex and are difficult to fully understand from field observations. Jardine & Standing (2000, 2012) reported results of multiple axial cyclic loading tests conducted on steel open-ended pipe piles driven in sand, at Dunkerque, northern France. The authors identified three kinds of responses (stable, unstable and meta-stable), depending on the mean shaft load, the shaft cyclic amplitude and the number of cycles. They also noted that a large number of low-level stable cycles can have beneficial effects on shaft capacity, whereas high-level cycles can lead to shaft failure and halving of the axial capacity within a few tens of cycles.

Numerous laboratory investigations have been reported on related topics of sand kinematics, grain crushing, local porosity changes and macroscopic interface behaviour (White & Bolton 2002, Yang et al. 2010, Silva et al. 2013, Arshad et al. 2014). The mechanisms controlling the macroscopic response of the interface were observed either *post-mortem* or in plane strain and mainly during pile installation.

The present work focuses on the sand grains behaviour in the vicinity of the pile during axial cyclic loading. The tests were performed in a mini-calibration chamber installed in an x-ray scanner. The pile was installed by jacking and submitted to 1000 displacement-controlled cycles under constant radial stress. The tests do not represent accurately real engineering applications, where piles supporting bridges, tidal or wind turbines are subjected to load-controlled cycles due to their environment. However, the macroscopic response of the sand-pile interface was compared and found to be consistent with the one obtained in a previous study using a pressurised calibration chamber (1.20 m internal diameter) conducted in the framework of a combined research effort by Laboratoire 3SR and Imperial College London (Tsuha et al. 2012, Silva 2014) in Grenoble, France. The consistency of the results shows their reproducibility for similar testing conditions at different scales of physical modelling. In addition, the combined use of three-dimensional (3D) tomographic imaging and advanced tools such as 3D-digital image correlation (3D-DIC), allows us to obtain quantitative information at the grain scale.

2 PHYSICAL MODEL

2.1 *Mini-calibration chamber and model pile*

The tests were carried out inside the x-ray scanner of Laboratoire 3SR. The mini-calibration chamber consists of a cylindrical cell transparent to x-rays in order to image phenomena while running a test (Fig. 1). The soil used for this study is Glageon sand, whose index properties are summarised in Table 1. Glageon sand is a calcareous sand derived from limestone rock crushed in Bocahut quarry, France, with $D_{50} = 1.125$ mm and a relatively uniform grading (between 1 mm and 1.25 mm).The angular and elongated shape of the grains of Glageon sand makes them highly crushable, which is the main reason they were selected for this study. The samples were prepared dry with an initial relative density ranging from 70% to 90%. At this relative density, triaxial compression tests gave φ' values of 48°.

An aluminium tubular model pile was used, with an external diameter of 14 mm. The pile tip was conical (60°) and instrumented with strain gauges to record pile tip resistance. A load cell was mounted on the pile head to measure the total load (or head load) applied on the pile. Shaft resistance was estimated by subtracting the tip load from the total load. The model pile had a smooth surface with a roughness of about 0.7 μm. The roughness of sand-pile interface is known to be one of the most important factors affecting the unit shaft resistance (Fioravante 2002, Hebeler et al. 2015, Tehrani et al. 2016). Therefore, in the present study, the friction mobilised by the shaft is lower than the one measured in the field. Direct shear tests on sand-aluminium interface gave $\delta' = 15°$ whereas field piles have a roughness that leads to a typical δ' of about $30°$.

2.2 *Pile installation and cyclic loading*

The pile was installed at a constant displacement rate of 25 μm/s until an initial embedment depth (either 50 or 60 mm) under a confining pressure of 100 kPa. For practical reasons, the pile was installed from the bottom of cell, i.e. it moves upwards. Following the installation, the pile was submitted to a thousand axial displacement-controlled cyclic loadings. The cycles were performed at the same displacement rate as for the installation with an amplitude of ±0.5 mm or ±1.0 mm, alternating between compression and tension phases (two-way cycles).

3 VISUALIZATION OF THE INTERFACE AND 3D-DIC

3D images were acquired throughout the cyclic loading after a certain number of cycles: 1, 50, 100, 500 and 1000 when the applied amplitude was ±0.5 mm.

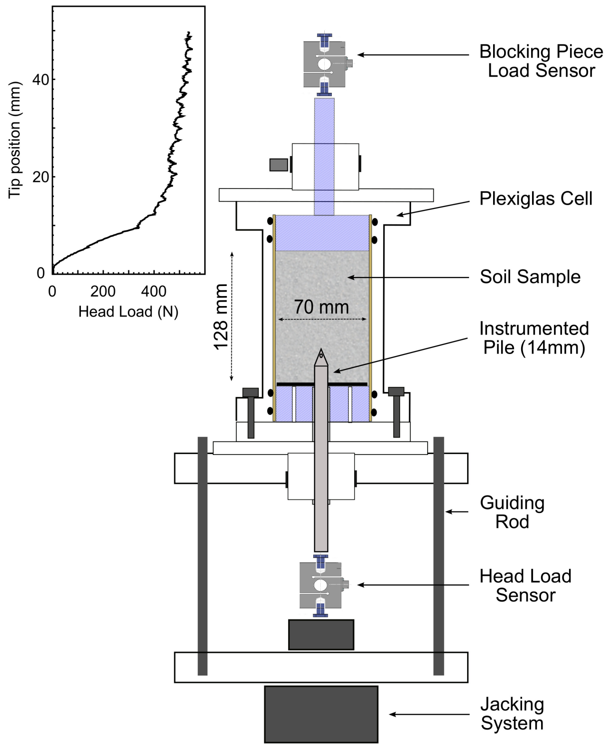

Figure 1. Schematic arrangement of the mini-calibration chamber and a typical head load profile during pile installation (top-left).

Restricted by the sample size, scans were taken in 'local' tomography, i.e. with a field of view focused on the tip and the shaft, for a voxel size of 40 μm (which means that there are about 25 voxels across a grain diameter). The x-ray beam was set to a tension of 150 kV and a current of 200 μA. Figure 2a shows a 3D rendering of the sand-pile interface after pile embedment.

3D fields of displacement and strain were obtained using the 3D-DIC code, TomoWarp2 (Tudisco et al. 2017). 3D-DIC is essentially a powerful tool for assessing the spatial transformation between two digital images, here tomographies. For fine sands, grains are too small with respect to voxel size and they cannot be tracked individually. However, a group of grains within a subdomain (containing about 8 grains in the present case), constitutes a speckle pattern and can be followed from one configuration to another. 3D-DIC was successfully used to study the installation of a pile in sand using the mini-calibration chamber (Silva & Combe 2014, Silva et al. 2015). The results, fully three-dimensional, showed distinct regions where the rearrangement of the grains concentrates. A 'recirculation' of sand grains was also observed close to the tip during the penetration of the pile.

In this work, a discrete version of TomoWarp2, developed at Laboratoire 3SR, was used, which allows for measuring the kinematics of each individual sand grain in the sample.

Table 1. Glageon sand properties

Grain shape	Volumetric weight	D_{50}	Coefficient of uniformity(C_u)	e_{max}	e_{min}
	kN/m^3	mm			
Angular	26.54	1.125	1.25	1.070	0.839

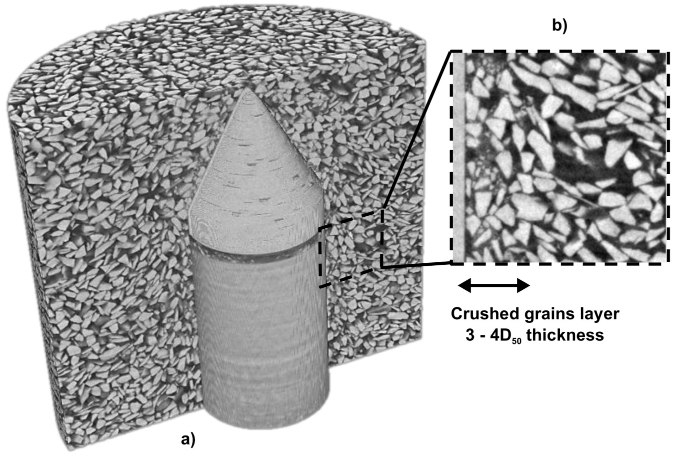

Figure 2. a) 3D rendering after pile installation inside the mini-calibration chamber. b) Zoom in the interface and detection of different phases (low grey level=pores, high grey level=grains, intermediate grey level=fines).

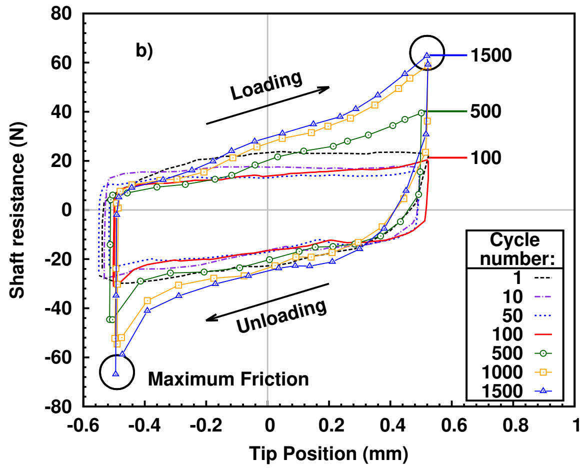

Figure 3. Mini-calibration chamber - Evolution of shaft resistance during cycles with an amplitude of ± 0.5 mm for GLAG-C1 (black arrows show the loading path).

4 RESULTS AND DISCUSSION

4.1 *Evolution of shaft resistance*

Figure 3 shows the shaft resistance during the cycles. Two different regimes can be identified. For the first 50 to 100 cycles, shaft resistance slightly decreases (of about 15 N), whereas it increases continuously and significantly for the subsequent load cycles. When the tip is at ± 0.5 mm the curves show a peak, which becomes increasingly marked with increasing number of cycles. As part of the national project SOLlicitations CYcliques sur Pieux de fondation (SOLCYP), Tali (2011) and Bekki et al. (2013) also reported an initial phase of 'cyclic softening' followed by a phase of 'cyclic hardening' for displacement-controlled cyclic loading tests carried out on a pile-probe jacked into large size samples of sand.

In the case of an amplitude of cycles of ± 1.0 mm the same trends as the one obtained for ± 0.5 mm can be observed but the transition between the two regimes occurs for a smaller number of cycles: between 10 to 20 cycles. These results suggest that reducing the imposed amplitude of displacement increases the number of cycles required to reach the increase in shaft resistance. From displacement-controlled calibration chamber model pile tests, Silva (2014) obtained similar results, as shown in Figure 4. The difference in the required number of cycles to pass from one regime to another is likely due to size effects regarding the ratio of the diameter of the chamber to the diameter of the pile as well as the ratio of the pile diameter to the mean particle size.

Figure 5 presents the force induced by friction measured at the peak for various tests performed on Glageon sand, in the mini-chamber, with identical testing parameters and similar relative density. The shaft resistance at the end of the cycles is twice as big as the value measured during the first cycle. The transition between the two regimes occurs at 50 to 100 cycles (shaded region in the figure).

4.2 *Grain kinematics*

In the following, only the results from test GLAG-C2 are shown, as the results from the other three tests are essentially the same. Typical fields of displacement from 3D-DIC are presented in Figure 6. Two pairs of 3D images were analysed, one from 10 to 50 cycles and one from 500 to 1000 cycles. It should be noted that these two increments respectively fall in the first and second regime of behaviour defined in Subsection 'Evolution of shaft resistance'. Cyclic loading induces significant displacements, mainly in the horizontal direction. Grains move globally towards the shaft for both loading steps leading to a significant radial contraction (Figs 6b, d). The sand mass undergoes very small vertical displacements - less than 20 μm (Figs 6a, c). In this study, sand grains tend to slide alongside the shaft (mainly due to the low roughness of pile shaft); however, relative displacements between grains, that is, rearrangement of the grains

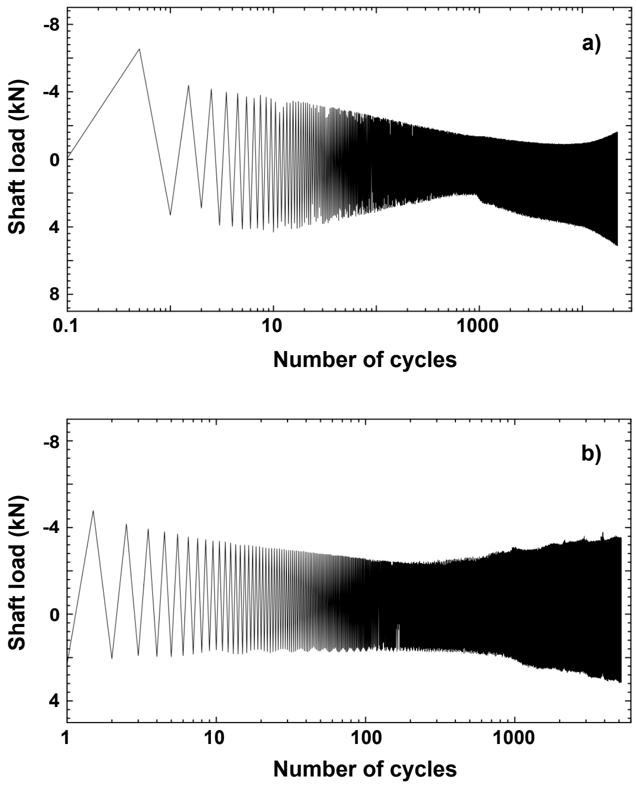

Figure 4. Large calibration chamber - Shaft load evolution during cyclic loading according to the applied amplitude of cycle (tests performed under constant confining pressure, Silva 2014): a) ± 0.5 mm, b) ± 1.0 mm.

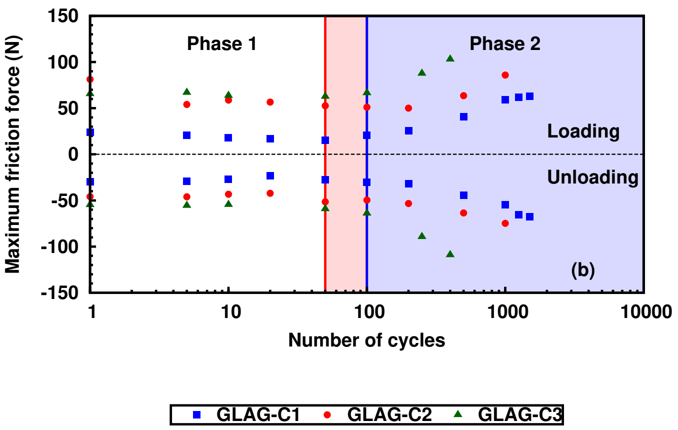

Figure 5. Mini-calibration chamber - Identification of two regimes in shaft resistance evolution (transition between 50 to 100 cycles noted by the shaded region).

occurs and is measured around the pile. By comparing vertical and horizontal displacement fields after 50 and 1000 cycles, two different behaviours can be observed. The first 50 cycles cause higher grain movements within a larger area around the shaft.

Individual displacement vectors for both loading increments are shown in Figures 5e, f. Ahead of the pile tip, the displacement vectors are nearly vertical and relatively minute, while around the shaft the displacement vectors have a much larger radial component. The displacement fields also reveal, in both increments, a thin layer around the shaft where the grains are highly disturbed and difficult to track from one image to another. In the first of the two increments shown, (Fig. 5e), grains are moving downwards. This is likely due to a reduction of the hoop stresses created during pile installation. This effect is erased in the later increment. More details about the grain kinematics analysis during cyclic loading can be found in Doreau-Malioche et al. 2018.

In addition to grain kinematics, discrete 3D-DIC proves to be a powerful tool offering a wide range of further possible analyses in terms of grain orientations, grain shape evolution and grain breakage quantification.

4.3 *Porosity Analysis*

X-ray images were analysed by studying the grey levels in order to quantitatively assess the effect of cycles on soil density (Desrues et al. 1996). The study was carried out by using the open source image processing software Fiji (Schindelin et al. 2012). Three phases were identified in the images as shown in Figure 2b: pores (low grey level), intact grains (high grey level) and fines produced by grain breakage. These fines are smaller than the pixel size, therefore, they cannot be resolved at the spatial resolution of the images. However, they can be associated with an intermediate mean grey level. Choosing an appropriate threshold, the percentage of voxels belonging to each phase was estimated within 5-voxels-thickness hollow cylinders centred on the pile axis. The radial evolution of the density of each phase during cyclic loading is plotted in Figure 7.

For one cycle, each point represents one measurement at a given distance from the shaft. The results show a significant increase in the percentage of voxels associated with intact grains (without taking fines into account) with increasing number of cycles. Close to the interface, the quantity of grains is 20% higher after 1000 cycles, which indicates a local densification at the interface. It can also be observed that the region affected is about $2D_{50}$ for Cycle 1 and $4D_{50}$ for Cycle 1000. In the rest of the sand mass, the proportion of grains and pores remains constant. This result indicates that the thickness of the band adjacent to the shaft is related to the displacements that the grains undergo and to the local shearing loading

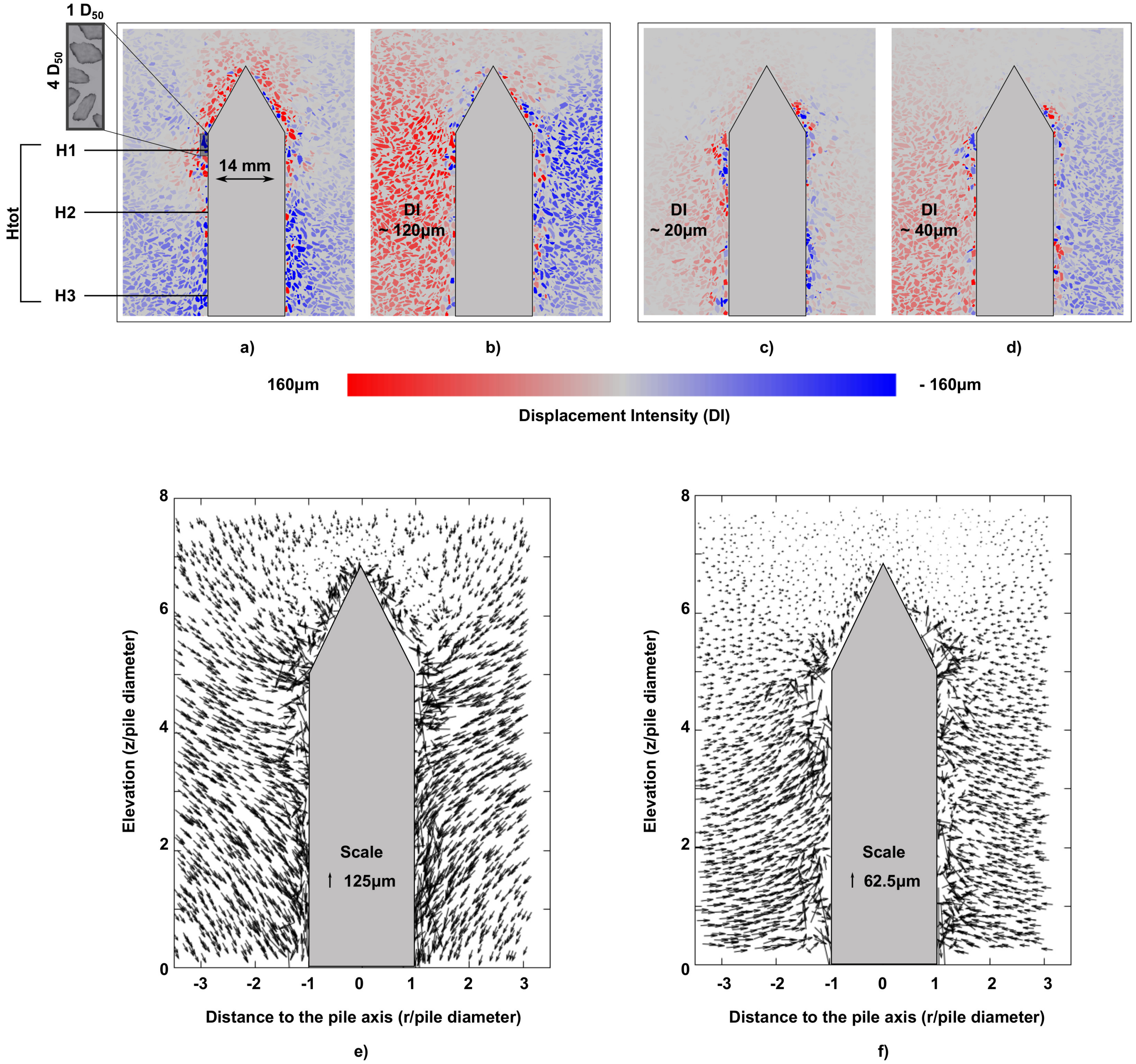

Figure 6. Typical individual grain displacements from discrete Digital Image Correlation (DIC), plotted in a vertical plane passing through the pile axis. Evolution of displacement intensity during cycles: a) vertical displacements, b) horizontal displacements between Cycle 10 and Cycle 50; c) vertical displacements, d) horizontal displacements between Cycle 500 and Cycle 1000. Individual displacement vectors e) between Cycle 10 and Cycle 50 and f) between Cycle 500 and Cycle 1000 (note that the scale is not the same for e) and f))

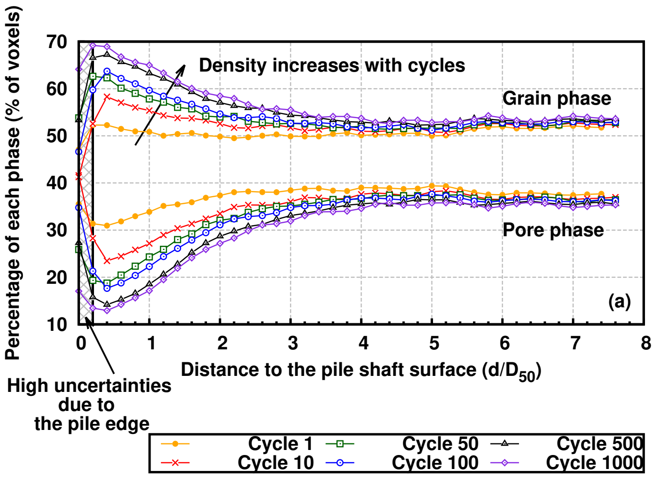

Figure 7. Local densification: radial evolution of intact grain (without fines) and pore phases during cycles for GLAG-C2 (scale: d=7D_{50}=0.5xpile radius). The two first data points should not be taken into account due to the effect of the edge of the pile on the images.

history. Yang et al. (2010) also report a shear zone $2 \cdot 4D_{50}$ $8 \cdot 6D_{50}$ wide, after cyclic jacking installation, in their large calibration chamber tests on NE34 Fontainebleau sand (D_{50}=0.21 mm). Similar to Silva et al. (2013), in their post-mortem analysis, Yang et al. (2010) suggest that the shear zone thickness grows with the vertical distance from the pile tip, especially when the installation is not monotonic, and is augmented by later static or cyclic loading.

5 CONCLUSIONS

X-ray tomography and 3D image analysis were used to investigate cyclic load effects on the sand-pile interface at the grain scale, within a mini-calibration chamber. Two distinct regimes were identified in the evolution of shaft resistance according to the number of applied cycles, with a non negligible increase of shaft resistance in the latter regime. For these two regimes, the measurement of grain kinematics revealed two different responses of the sand mass associated with a significant densification at the interface.

In this experimental study, the test conditions are admittedly not representative of true field conditions. In fact, some of the results obtained in this study cannot (and should not) be directly extrapolated to field cases. For example, the positive effect of cyclic loading on shaft resistance is a clear consequence of the very specific way loading cycles are applied (full failure displacement-controlled) which is rarely the case in the field. However, the macroscopic response of the interface in the mini-calibration chamber is consistent with the one obtained in a previous study carried out at a larger scale within the large calibration chamber of Laboratoire 3SR. These results indicate that the size effects do not affect the main mechanisms occurring at the grain scale and controlling the macroscopic behaviour of the sand-pile interface. The small scale study offers new possibilities in terms of quantitative analysis of the behaviour of the sand grains at the interface.

A second experimental campaign, conducted under constant normal stiffness, would provide further results that could be compared to the ones obtained for field tests.

6 ACKNOWLEDGEMENTS

The authors gratefully acknowledge Pascal Charrier, Christophe Dano and Edward Andò, all from Laboratoire 3SR, for their contributions. Laboratoire 3SR is part of the LabEx Tec 21 (Investissements dAvenir grant agreement number ANR-11-LABX-0030).

REFERENCES

Arshad, M. F., Tehrani, S. Prezzi, M. & Salgado, R. (2014). Experimental study of cone penetration in silica sand using digital image correlation. *Géotechnique 64 (7)*, 551–569.

Bekki, H., Canou, J., Tali, B., Dupla, J. C. & Bouafia, A. (2013). Evolution of local friction along a model pile shaft in a calibration chamber for a large number of loading cycles. *Comptes Rendus Mcanique 341 (6)*, 499–507.

Desrues, J., Chambon, R., Mokni, M. & Mazerolle, F. (1996). Void ratio evolution inside shear bands in triaxial sand specimens studied by computed tomography. *Géotechnique 46 (3)*, 529–546.

Doreau-Malioche, J., Combe, G., Viggiani, G. & Toni, J. B. (2018). Shaft friction changes for cyclically loaded displacement piles: an x-ray investigation. *Géotechnique Letters*, DOI: 10.1680/jgele.17.00141.

Fioravante, V. (2002). On the shaft friction modelling of non-displacement piles in sand. *Soils Found. 42 (2)*, 23–33.

Hebeler, G. L., Martinez, A. & Frost, J. D. (2015). Shear zone evolution of granular soils in contact with conventional and textured CPT friction sleeves. *KSCE J. Civil Engng. 20 (4)*, 1267–1282.

Jardine, R. J. & Standing, J. R. (2000). Pile load testing performed for HSE cyclic loading study at Dunkirk, France, Vols 1 and 2. *SOffshore Technology Report OTO 2000 007* London, UK: Health and Safety Executive, two volumes 60p, 200p.

Jardine, R. J. & Standing, J. R. (2012). Field axial cyclic loading experiments on piles driven in sand. *Soils Found. 52 (4)*, 723–737.

Schindelin, J., Arganda-Carreras, I. & Frise, E. (2012). Fiji: an open-source platform for biological-image analysis. *Nature methods 9 (7)*, 676–682, PMID 22743772, doi:10.1038/nmeth.2019.

Silva, M. (2014). Experimental study of ageing and axial cyclic loading effect on shaft friction along driven piles in sand. *PhD Thesis*, Université de Grenoble, France.

Silva, M. & Combe, G. (2014). Sand displacement field analysis during pile installation using x-ray tomography and digital image correlation. *International Symposium on Geomechanics from Micro to Macro, Cambridge, UK*, CRC Press/Balkema, vol. 1, pp. 15991603.

Silva, M., Combe, G., Foray, P., Flin, F. & Lesaffre, B. (2013). Postmortem Analysis of Sand Grain Crushing From Pile Interface Using X-ray Tomography. In *AIP Conf. Proc. Powders and Grains, Sydney, Australia*. UNSW, vol. 1542, pp. 297-300.

Silva, M., Doreau-Malioche, J. & Combe, G. (2015). Champs cinématiques dans un sable lors de l'enfoncement d'un pieu par tomographie RX: comparaison des corrélations numériques continue et discrète. *22me Congrès Français de Mécanique*, Lyon, France.

Tali, B. (2011). Comportement de l'interface sols-structure sous sollicitations cycliques : application au calcul des fondations profondes. *PhD Thesis*, Université de Paris Est, France.

Tehrani, F. S., Han, F., Salgado, R., Prezzi, M., Tovar, R. D. & Castro, A. G. (2016). Effect of surface roughness on the shaft resistance of non-displacement piles embedded in sand. *Géotechnique 66 (5)*, 386–400.

Tsuha, C. H. C., Foray, P. Y., Jardine, R. J., Yang, Z. X., Silva, M. & Rimoy, S. (2012). Behaviour of displacement piles in sand under cyclic axial loading. *Soils Found. 52 (3)*, 393–410.

Tudisco, E., Andò, E., Cailletaud, R. & Hall, S. A. A local Digital Volume Correlation code. *SoftwareXC 6*, 267–270.

White, D., & Bolton, M. (2002). Observing friction fatigue on a jacked pile. In Springman S. M. (ed.) *Constitutive and Centrifuge Modeling: Two Extremes*, Rotterdam/Balkema, pp. 347354.

Yang, L., Jardine, R., Zhu, B., Foray, P. & Tsuha, C. (2010). Sand grain crushing and interface shearing during displacement pile installation in sand. *Géotechnique 60 (6)*, 469–482.